Onset of chaos in Josephson junctions with intermediate damping

X. Yao,* J. Z. Wu, and C. S. Ting
Texas Center for Superconductivity and Department of Physics, University of Houston, Houston, Texas 77204
(Received 13 July 1989; revised manuscript received 28 February 1990)

By use of the analytical solution of the Stewart-McCumber equation including quadratic damping and dc bias, the Melnikov method has been extended to the parameter regions of intermediate damping and dc bias for the Josephson junctions with quadratic damping and with linear damping and cosϕ term. The comparison between the thresholds predicted by the Melnikov method and that derived from numerical simulation has been studied. In addition, the validity conditions for the Melnikov threshold are also discussed.

I. INTRODUCTION

The existence of chaos in a Josephson junction driven by rf-biased current has been verified through the theory, simulation, and experiment. The extensive study on chaos in this system is partly due to the fact that when we treat the Josephson junction within the Stewart-McCumber model, the equation of motion is one of the simplest to exhibit chaos and describes a significant physical system. In terms of dimensionless parameters, the equation of motion for the phase difference ϕ in a current-driven Josephson junction is given by

$$d^2\phi/d\tau^2+\alpha(1+\delta\cos\phi)d\phi/d\tau+\sin\phi=\rho_0+\rho_1\sin(\Omega\tau)\ , \tag{1}$$

where $\alpha=(\hbar/2eI_cR^2C)^{1/2}$ is the damping constant, $\rho_0=I_0/I_c$ is the normalized dc bias, $\rho_1=I_1/I_c$ is the normalized rf amplitude, $\Omega=\omega(\hbar C/2eI_c)^{1/2}$ is the normalized rf frequency, and $\tau=t(2eI_c/\hbar C)^{1/2}$ is the normalized time. The minimum rf amplitude required to produce chaos has been previously investigated[1-5] in terms of the Melnikov method. In those works the unperturbed equation was usually chosen to be conservative, i.e.,

$$d^2\phi/d\tau^2+\sin\phi=0\ . \tag{2}$$

According to the Melnikov method, the necessary condition for the onset of chaos is $\rho_1>\rho_{1\text{th}}$ with the threshold value $\rho_{1\text{th}}$ defined as

$$\rho_{1\text{th}}=\left|\pm\rho_0-\frac{4\alpha}{\pi}(1+\delta/3)\right|\cosh(\pi\Omega/2)\ . \tag{3}$$

The threshold given by the Melnikov method is expected[1] to be accurate only in the parameter regions where the perturbed equation represents a nearly conservative system. This implies that the maximum energy change caused by the dissipation or the current source within one excursion of the heteroclinic orbit is much smaller than the total energy of the unperturbed system. For $\delta=0$, these conditions can be written as[1]

$$\alpha\ll\tfrac{1}{4},\ \ \rho_0\ll1/\pi,\ \text{and}\ \Omega<1\ . \tag{4}$$

For the rf amplitude ρ_1, Kautz and Macfarlane[1] argued that it is not possible to obtain a simple expression for the energy supplied by the rf source therefore they assumed a condition similar to that for the dc bias, i.e.,

$$\rho_1\ll1/\pi\ . \tag{5}$$

In this work we are discussing the problem of the onset of chaos in a Josephson junction with an intermediate damping constant, which means that α is of the order of unity. Thus the condition $\alpha\ll\frac{1}{4}$ is no longer satisfied and treating the damping term in Eq. (1) as a perturbation is not proper. However, if the damping term and the corresponding dc bias are included into the unperturbed equation, which is

$$d^2\phi/d\tau^2+\alpha(1+\delta\cos\phi)d\phi/d\tau+\sin\phi=\rho_0\ , \tag{6}$$

no analytical solution can be found to calculate the Melnikov function of Eq. (1).

Instead of solving Eq. (6) we are using a solvable equation

$$d^2\phi/d\tau^2+\gamma|d\phi/d\tau|d\phi/d\tau+\sin\phi=\rho_0\ , \tag{7}$$

as the unperturbed system of Eq. (1). The only difference between Eq. (6) and Eq. (7) is the damping term. However, we can treat this difference as a perturbation as long as it is small enough. Equation (7) is also based on the Steward-McCumber model with the normal resistance depending on voltage, $R=\text{const}/V$.[6] A lot of interest has recently been attracted to this system because it provides a better agreement with experimentally measured I-V curves than the linear damping at high temperature and a simple model to display the nonlinear behavior in the Josephson junction.[7] Therefore, in Sec. II we are going to discuss the application of the Melnikov method to the Josephenson junction with quadratic damping including both small and intermediate damping cases. In Sec. III we will use Eq. (7) as the unperturbed system to discuss the onset of chaos in the Josephson junction with linear damping and the cosϕ term. As a comparison, the onset of chaos in Josephson junctions will also be studied by numerical simulation. Section IV contains the conclusion and discussion.

II. THE JOSEPHSON JUNCTION WITH QUADRATIC DAMPING

In order to elucidate the following discussion, we briefly review the Melnikov method.[8] Consider a system described by an ordinary differential equation of the form

$$d\mathbf{x}/dt=\mathbf{h}_0(\mathbf{x})+\epsilon\mathbf{h}_1(\mathbf{x},t)\ , \tag{8}$$

where $\epsilon\mathbf{h}_1$ is the perturbation. If the unperturbed equation of Eq. (8) has an analytical solution, the Melnikov function can be calculated according to the definition

$$M(t_0)=\int_{-\infty}^{\infty}\mathbf{h}_0[\mathbf{x}_h(t-t_0)]\times\mathbf{h}_1[\mathbf{x}_h(t-t_0),t] \times\exp\left[-\int_0^{t-t_0}\mathrm{tr}\{D_{\mathbf{x}}\mathbf{h}_0[\mathbf{x}_h(s)]\}ds\right]dt\ , \tag{9}$$

where $\mathbf{x}_h$ denoted the homoclinic orbit or heteroclinic orbit of the unperturbed system, $\mathbf{x}\times\mathbf{y}$ is defined as the outer product of $\mathbf{x}$ and $\mathbf{y}$, and $D_{\mathbf{x}}$ denotes the partial derivative with respect to $\mathbf{x}$. If $M(t_0)$ has a simple zero and is independent of ϵ, the local stable and unstable manifolds intersect transversally. The presence of such transversal intersections implies that the Poincaré map has the so-called Smale-horseshoe chaos.

The equation of the current-driven Josephson junction with quadratic damping can be written as[6]

$$d^2\phi/d\tau^2+\gamma|d\phi/d\tau|d\phi/d\tau+\sin\phi=\rho_0+\rho_1\sin(\Omega\tau)\ . \tag{10}$$

The unperturbed system may be chosen in two different ways:

(i) *The conservative system.* In this case, the unperturbed equation is chosen to be Eq. (2) which has the heteroclinic orbit

$$\begin{aligned}\phi_h(\tau-\tau_0)&=\pm2\tan^{-1}[\sinh(\tau-\tau_0)]\ ,\\ y_h(\tau-\tau_0)&=\pm2\,\mathrm{sech}(\tau-\tau_0)\ ,\end{aligned} \tag{11}$$

and the energy integral,

$$E_h=\tfrac{1}{2}y_h^2+1-\cos\phi_h=2\ . \tag{12}$$

Here $y\equiv d\phi/d\tau$ and the subscript h represents the heteroclinic orbit. From this unperturbed heteroclinic orbit, the Melnikov function of Eq. (10) can be obtained[7] as

$$M(\tau_0)=\pm2\pi\rho_0\pm2\pi\rho_1\,\mathrm{sech}(\pi\Omega/2)\sin(\Omega\tau_0)-4\pi\gamma\ , \tag{13}$$

and the necessary condition for the onset of chaos is $\rho_1>\rho_{1\mathrm{th}}$, with $\rho_{1\mathrm{th}}$ defined as

$$\rho_{1\mathrm{th}}=|\pm\rho_0+2\gamma|\cosh(\pi\Omega/2)\ . \tag{14}$$

For convenience, we call it conservative threshold. This threshold is expected to be accurate only in the parameter region where Eq. (10) represents a nearly conservative system. In other words, the energy fluctuation should be very small. Within one excursion of the heteroclinic orbit, the maximum change of energy due to the dissipation is

$$E_d^M=\int_{-\pi}^{\pi}\gamma y_h^2 d\phi_h=4\pi\gamma\ , \tag{15}$$

and the maximum energy supplied by the dc source is

$$E_{\mathrm{dc}}^M=\int_{-\pi}^{\pi}\rho_0 d\phi_h=2\pi\rho_0\ . \tag{16}$$

The requirement of E_d^M and E_{dc}^M being smaller than the total energy of the unperturbed system Eq. (12) gives

$$\gamma\ll\frac{1}{2\pi}\ \text{and}\ \rho_0\ll1/\pi\ . \tag{17}$$

For the rf source, instead of using Eq. (5) which seems too strict for large Ω, we suggest another condition which is frequency dependent:

$$\rho_1\ll\rho_{1c}=\left[\int_{-\pi/2\Omega}^{\pi/2\Omega}d\tau\cos(\Omega\tau)\,\mathrm{sech}(\tau)\right]^{-1}\ . \tag{18}$$

The reason for such a choice is given below: the energy supplied (or extracted) by the rf source during any time interval $[a,b]$ along the heteroclinic orbit can be written as

$$|E_{\mathrm{rf}}|=\left|2\rho_1\int_a^b\mathrm{sech}(\tau)\sin[\Omega(\tau+\tau_0)]d\tau\right|\ . \tag{19}$$

We already know that $\mathrm{sech}(\tau)$ is symmetric about $\tau=0$ and monotonic on each side. It is positive definite and has the maximum value 1 at $\tau=0$. Thus if we choose $\tau_0=\pm(2n+1)\pi/2\Omega$ (here n is an arbitrary integer) and integrate over the interval $(-\pi/2\Omega,\pi/2\Omega)$ within which the $\sin[\Omega(\tau+\tau_0)]$ is positive or negative definite, we have the maximum value E_{rf}^M for $|E_{\mathrm{rf}}|$, i.e.,

$$|E_{\mathrm{rf}}|\le E_{\mathrm{rf}}^M=|2\rho_1|\int_{-\pi/2\Omega}^{\pi/2\Omega}\mathrm{sech}(\tau)\cos(\Omega\tau)d\tau\ . \tag{20}$$

Requiring $E_{\mathrm{rf}}^M\ll E_h$, we arrive at Eq. (18). It is easy to see that if Ω approaches zero, the inequality (18) returns to Eq. (5), but for finite Ω it is less restrictive since ρ_{1c} increases monotonically with Ω (see also Fig. 2).

(ii) *The dissipative system.* The unperturbed system of Eq. (10) may also be chosen to be Eq. (7) which is obviously a dissipative system. When ρ_0 takes the value $\rho_c=2\gamma/(4\gamma^2+1)^{1/2}$, we have the heteroclinic orbit for Eq. (7) (Ref. 7)

$$\begin{aligned}\phi_h(\tau-\tau_0)&=4\tan^{-1}\{\exp[b(\tau-\tau_0)/2]\}-\beta-\pi\ ,\\ y_h(\tau-\tau_0)&=b\,\mathrm{sech}[b(\tau-\tau_0)/2]\ ,\end{aligned} \tag{21}$$

where $b=(2\rho_c/\gamma)^{1/2}$ and $\tan\beta=2\gamma$. For Eq. (7) the Melnikov function of Eq. (10) and the necessary condition for the onset of chaos have been previously obtained.[7] The Melnikov function is

$$M(\tau_0)=(\rho_0-\rho_c)\sin(2\pi\gamma)/\gamma+\rho_1 b[F_1\cos(\Omega\tau_0)+F_2\sin(\Omega\tau_0)]\ , \tag{22}$$

where

$$F_1=\int_{-\infty}^{\infty}\mathrm{sech}(b\tau/2)\sin(\Omega\tau)\times\exp\{4\gamma\tan^{-1}[\sinh(b\tau/2)]\}d\tau\ , \tag{23}$$

$$F_2=\int_{-\infty}^{\infty}\mathrm{sech}(b\tau/2)\cos(\Omega\tau)\times\exp\{4\gamma\tan^{-1}[\sinh(b\tau/2)]\}d\tau\ . \tag{24}$$

The necessary condition for the onset of chaos is $\rho_1 > \rho_{1\text{th}}$, where $\rho_{1\text{th}}$ is defined as

$$\rho_{1\text{th}} = |\rho_0 - \rho_c| \sinh(2\pi\gamma)/\gamma b (F_1^2 + F_2^2)^{1/2} . \quad (25)$$

We call it dissipative threshold. Since the total average energy change in Eq. (7) over one excursion of the heteroclinic orbit is equal to zero

$$\int_{-\infty}^{\infty} (\rho_c - \gamma y_h^2) y_h d\tau = \int_{-\beta-\pi}^{-\beta+\pi} (\rho_c - \gamma y_h^2) d\phi_h = 0 , \quad (26)$$

and we may introduce an average energy E_{av} of the system over one excursion of the heteroclinic orbit, which is defined as

$$E_{\text{av}} = (1/2\pi) \int_{-\beta-\pi}^{-\beta+\pi} [y_h^2/2 + 1 - \cos(\phi_h)] d\phi_h$$
$$= 1 + 1/(4\gamma^2+1)^{1/2} . \quad (27)$$

The mean-square root of the energy derivation ΔE_{msr} on the heteroclinic orbit is

$$\Delta E_{\text{msr}} = \left[(1/2\pi) \int_{-\beta-\pi}^{-\beta+\pi} \{ [y_h^2/2 + 1 - \cos(\phi_h)] - E_{\text{av}} \}^2 d\phi_h \right]^{1/2}$$
$$= \sqrt{2}\gamma/(4\gamma^2+1)^{1/2} . \quad (28)$$

From Eqs. (27) and (28), we can easily see that $\Delta E_{\text{msr}} \ll E_{\text{av}}$ for $\gamma \leq 1$. Therefore, in the case of intermediate damping the average energy can be used as a characteristic quantity of the unperturbed system to estimate the relative change of energy in the perturbed system. Over one excursion of the heteroclinic orbit the maximum amount of energy supplied (or extracted) by the perturbative dc source is

$$E_{\text{dc}}^M = \left| \int_{-\infty}^{\infty} (\rho_0 - \rho_c) y_h d\tau \right| = 2\pi |\rho_0 - \rho_c| . \quad (29)$$

Similarly, the maximum amount of energy supplied (or extracted) by the rf source is

$$E_{\text{rf}}^M = |b\rho_1| \int_{-\pi/2\Omega}^{\pi/2\Omega} \text{sech}(b\tau/2)\cos(\Omega\tau) d\tau . \quad (30)$$

Requiring E_{dc}^M and E_{rf}^M to be smaller than E_{av} yields

$$2\pi|\rho_0 - \rho_c| \ll 1 + 1/(4\gamma^2+1)^{1/2} , \quad (31)$$

and

$$\rho_1 \ll \rho_{1c} = \frac{[1 + 1/(4\gamma^2+1)^{1/2}]}{\left[b \int_{-\pi/2\Omega}^{\pi/2\Omega} d\tau \text{sech}(b\tau/2)\cos(\Omega\tau) \right]} . \quad (32)$$

Equations (31) and (32) represent the validity conditions for the Melnikov threshold given by Eq. (25).

It would be very interesting to understand the difference between Melnikov functions calculated for these two different unperturbed systems. When $\rho_0 = 0$, it is easy to see that there is no significant difference between these two cases. For the conservative unperturbed system we only have the condition $\gamma \ll 1/2\pi$ from Eq. (17) because of the absence of dc bias. For the dissipative case, the perturbation has the form of $[-\rho_c + \rho_1 \sin(\Omega\tau)]$. Using Eq. (31) with $\rho_0 = 0$, we have

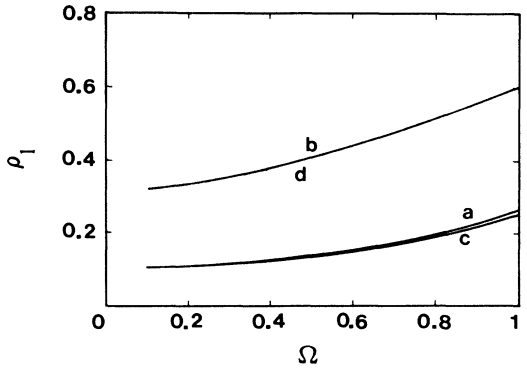

FIG. 1. Quadratic damping: the Melnikov threshold $\rho_{1\text{th}}$ and the validity condition ρ_{1c} for $\gamma = 0.1$ and $\rho_0 = 0$. (a) $\rho_{1\text{th}}$ and (b) ρ_{1c} based on the conservative system. (c) $\rho_{1\text{th}}$ and (d) ρ_{1c} based on the dissipative system. (b) and (d) coincide with each other.

$$\gamma \ll \gamma_c = 2\pi/(4\pi^2 - 1) \simeq 1/2\pi \approx 0.16 . \quad (33)$$

Comparing Eqs. (17) and (33), it is evident that the conditions satisfied by damping constant γ are almost the same for both choices of the unperturbed system.

In Fig. 1, the comparison between these two Melnikov thresholds is shown in $\Omega - \rho_1$ plane with $\gamma = 0.1$ and $\rho_0 = 0$. It is obvious that two $\rho_{1\text{th}}$ curves as well as two ρ_{1c} curves coincide very well. If $\gamma > \gamma_c \simeq 0.16$, the conditions (17) or (33) which guarantee the validity of the conservative or dissipative threshold, respectively, is no longer satisfied. We do not expect that the Melnikov method could still give a good prediction with such a large perturbation. Therefore, there is no substantial improvement for the Melnikov method based on the dissipative unperturbed system when it is compared with the result on the conservative one in the case of only rf-biased current or $\rho_0 = 0$. Actually, we will show in Fig. 3 that this statement is still correct if both the dc bias and the damping constant are very small.

The situation becomes quite different when $\rho_0 \neq 0$ and γ is not very small. One may notice that dc bias ρ_0 must be chosen near the value of ρ_c because of the condition in Eq. (31). In Fig. 2, two thresholds calculated from Eq.

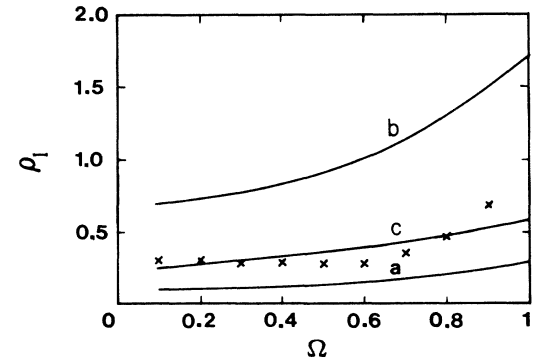

FIG. 2. Quadratic damping: onset of chaos for $\gamma = 0.7$ and $\rho_0 - \rho_c = -0.1$. (a) The dissipative threshold; (b) the conservative threshold; (c) the validity condition ρ_{1c} according to Eq. (32); crosses—onset of chaos from the numerical simulation.

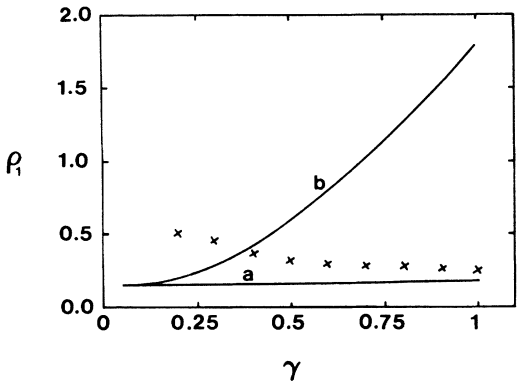

FIG. 3. Quadratic damping: onset of chaos for $\Omega=0.6$ and $\rho_0-\rho_c=-0.1$. The notation here is the same as that in Fig. 2.

(25) and Eq. (14) are shown on the ρ_1-Ω plane with $\gamma=0.7$ and $(\rho_0-\rho_c)=-0.1$. The validity condition Eq. (32) is also plotted in Fig. 2. To make a comparison, the chaotic behavior of Eq. (10) has been investigated numerically. In our numerical simulations, the lower boundary of the chaos threshold is determined by following the successive bifurcation of the trajectories (see Sec. III for details) and by recording the first appearance of a positive Liapunov exponent[8] with increasing the rf amplitude ρ_1. From Fig. 2 it is evident that the numerical threshold of ρ_1 is above and very close to the dissipative threshold especially for $0.3<\Omega<0.8$; there the rf bias is below ρ_{1c}. We also noticed that the conservative threshold cannot be used to predict the chaos since it is too high to compare with the result of numerical simulation. Therefore it has been verified that the Melnikov method based on the dissipative unperturbed system can give a good estimation of the chaos criterion for a Josephson junction with intermediate damping.

In Fig. 3, the comparison is shown in γ-ρ_1 plane where we fix $\Omega=0.6$, $\Delta\rho_0=\rho_0-\rho_c=-0.1$. It is easy to see that the dissipative and conservative thresholds diverge from one another with the damping constant γ. Meanwhile the numerical threshold approaches the dissipative threshold and the two curves seem to coincide for large γ. This implies that the dissipative threshold can be used as the criterion for chaos of Eq. (10) in the parameter region where the damping constant is greater than $\gamma_1=0.32$ and the dc bias is around the critical value ρ_c. However, for $\gamma<\gamma_1$, the conservative threshold is a better predictor. But there is still a noticeable discrepancy between the Melnikov prediction and the numerical result. We should also point out that the two Melnikov thresholds almost join together when γ is below $1/2\pi$ as we already mentioned previously.

III. JOSEPHSON JUNCTIONS WITH LINEAR DAMPING AND cosϕ TERM

In this section we discuss the onset of chaos of a Josephson junction with linear damping and a cosϕ term [see Eq. (1)]. The cosϕ term, which represents the current through the junction due to interference between the quasiparticles and Cooper pairs, is often neglected when studying the nonlinear dynamic behavior of the junction within the Stewart-McCumber model. However, the cosϕ term actually has played an important role in explaining the experimental results of a Josephson junction radiated by microwave in the famous work of Pedersen, Finnegan, and Langenberg.[9] Generally, current flowing through the Josephson junction contains a cosϕ term.

It is essential to know the heteroclinic orbit of an unperturbed system for the application of the Melnikov method. In the case of intermediate damping, we choose Eq. (7) as the unperturbed system and its heteroclinic orbit has already been given by Eq. (21). Comparing Eq. (1) with Eq. (7), we can write the perturbation in Eq. (1) as follows:

$$\gamma|d\phi/d\tau|d\phi/d\tau-\alpha(1+\delta\cos\phi)d\phi/d\tau+(\rho_0-\rho_c)+\rho_1\sin\Omega\tau\ . \tag{34}$$

Here the free parameter γ can be chosen in such a way as to "kill" the secular term in the perturbation, which means that the average of Eq. (34) on the heteroclinic orbit Eq. (7) is set to be zero, i.e.,

$$\int_{-\infty}^{\infty} d\tau[\gamma y_h^2(\tau)-\alpha(1+\delta\cos\phi_y)y_h(\tau)+(\rho_0-\rho_c)]y_h(\tau)=2\pi\rho_0-8\alpha(1+\delta/3\sqrt{1+4\gamma^2})/\sqrt[4]{1+4\gamma^2}=0\ . \tag{35}$$

Equation (35) is a third-order polynomial equation of $z\equiv 1/\sqrt[4]{1+4\gamma^2}$. It has a real and positive solution for γ only if $\rho_0/\alpha\le 8/3\pi|\delta|$, which is

$$\gamma=\frac{1}{2}\left[\frac{1}{z^4}-1\right]^{1/2},$$
$$z=2\sqrt[3]{r}\cos\left[\theta+\frac{4\pi}{3}\right], \tag{36}$$
$$r=\frac{1}{\sqrt[3/2]{|\delta|}},\quad \theta=\tfrac{1}{3}\cos^{-1}\left[-\frac{3\pi\rho_0\sqrt{|\delta|}}{8\alpha}\right].$$

Then the Melnikov function of Eq. (1) can be obtained from Eq. (9)

$$M(\tau_0)=\int_{-\infty}^{\infty} y_h(\tau)\{\gamma y_h^2(\tau)-\alpha[1+\delta\cos\phi_h(\tau)]y_h(\tau)+(\rho_0-\rho_c)+\rho_1\sin[\Omega(\tau-\tau_0)]\}\exp\{4\gamma\tan^{-1}[\sinh(b\tau/2)]\}d\phi$$
$$=C\sinh(2\pi\gamma)-D\cosh(2\pi\gamma)+\rho_1 b[F_1\cos(\Omega\tau_0)+F_2\sin(\Omega\tau_0)] , \quad (37)$$

where F_1 and F_2 are previously defined by Eqs. (23) and (24), and

$$C=(\rho_0-\rho_c)/\gamma+b^2/2(4\gamma^2+1) , \quad (38)$$

$$D=b\alpha\delta[(12-64\gamma^2)\cos\beta+64\gamma\sin\beta]/[(16\gamma^2+1)(16\gamma^2+9)]+4b\alpha/(16\gamma^2+1) . \quad (39)$$

The necessary condition for the function $M(\tau_0)$ in Eq. (37) to be zero is $\rho_1>\rho_{1\text{th}}$, where the chaos threshold $\rho_{1\text{th}}$ is

$$\rho_{1\text{th}}=|C\sinh(2\pi\gamma)-D\cosh(2\pi\gamma)|/b(F_1^2+F_2^2)^{1/2} . \quad (40)$$

As in Sec. II, we refer the expression in Eq. (40) and Eq. (3), respectively, as the dissipative and conservative thresholds. In order to make a comparison between those two thresholds, we have also investigated the onset of chaos numerically by following the successive bifurcation of the trajectory and calculating the Liapunov exponent. In Figs. 4 and 5, the typical ways to chaos through period doubling from the phase-locked rotation-

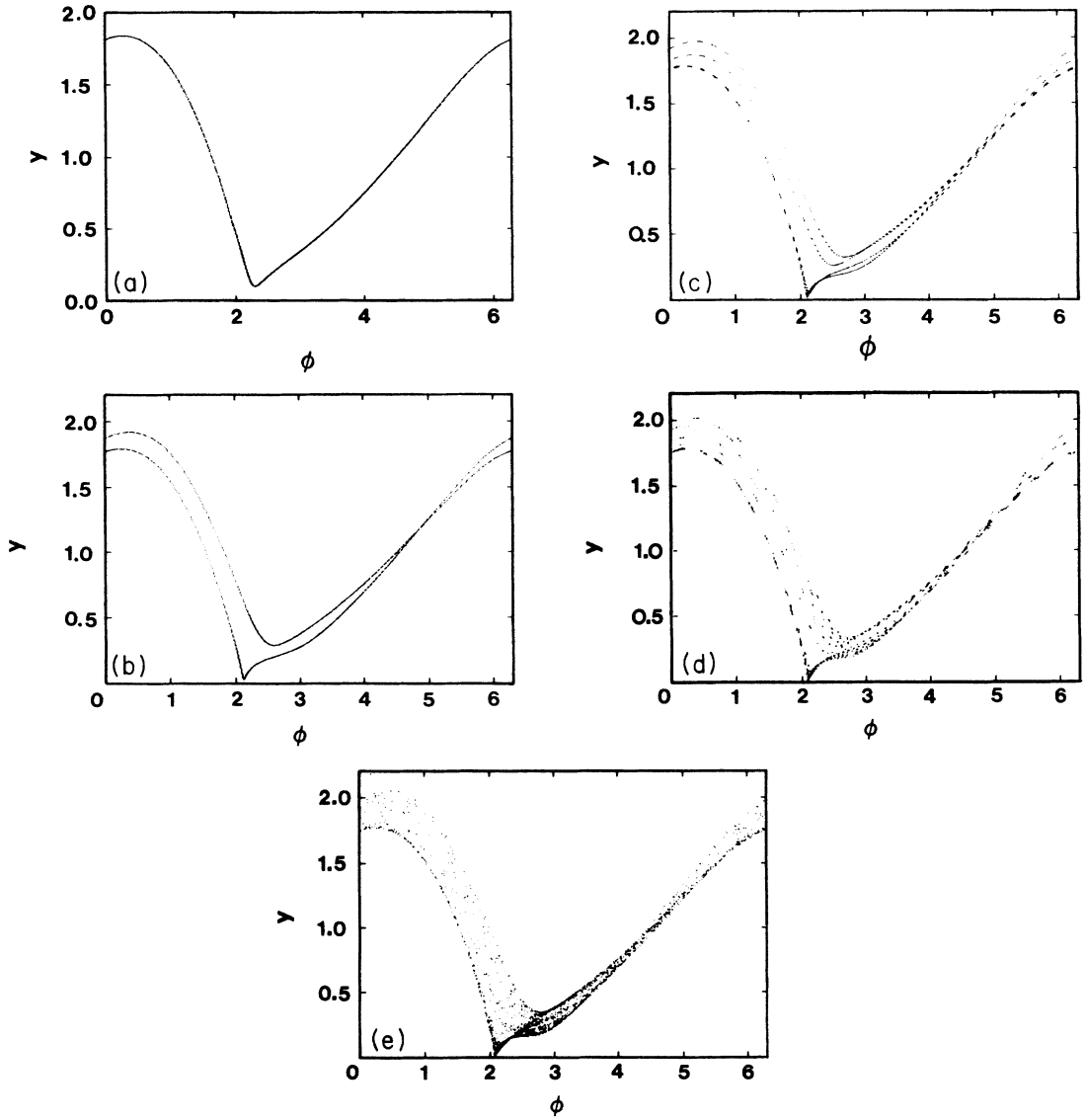

FIG. 4. Linear damping with the $\cos\phi$ term: rotational orbit for $\Omega=0.6$, $\alpha=1.004\,25$, $\delta=-0.8$, and $\rho_0=0.823\,733$. (a) Period 1 orbit for $\rho_1=0.12$; (b) period 2 orbit for $\rho_1=0.18$; (c) period 4 orbit for $\rho_1=0.185$; (d) and (e) chaotic orbits for $\rho_1=0.195$ and $\rho_1=0.2$.

al and oscillational trajectories are shown in phase space respectively for $\Omega=0.6$, $\alpha=1.004$, and $\rho_0=0.8237$. To avoid the transient behavior, we started to take points after throwing away about 1000 cycles of $T=2\pi/\Omega$. Each trajectory is composed of 2000 points with the time interval $\Delta\tau=\tau_{i+1}-\tau_i$ between two adjacent points being set equal to 1. Also, we take mod2π of ϕ. In Fig. 4 the initial point is chosen to be (3, 0.25) in the phase space. For $\rho_1=0$, the stable rotational orbit has period $T_0=2\pi/\Omega$ with $\Omega_0=0.6873$ [Fig. 4(a)]. For $\rho_1>0.04$, the orbit becomes phase-locked with period $T=2\pi/\Omega$ [see Fig. 4(b)]. As ρ_1 increases from 0.12 to 0.195, the trajectory experiences a process of period-doubling to chaos. On the other hand, if we start from (1,0), the trajectory is still phase-locked for rf bias below 0.4, but the motion is oscillational [see Fig. 5(a)]. As ρ_1 increases from 0.4, the orbit again goes through the period-doubling bifurcation and becomes chaotic at $\rho_1=0.45$ [see Fig. 5(b) and 5(c)].

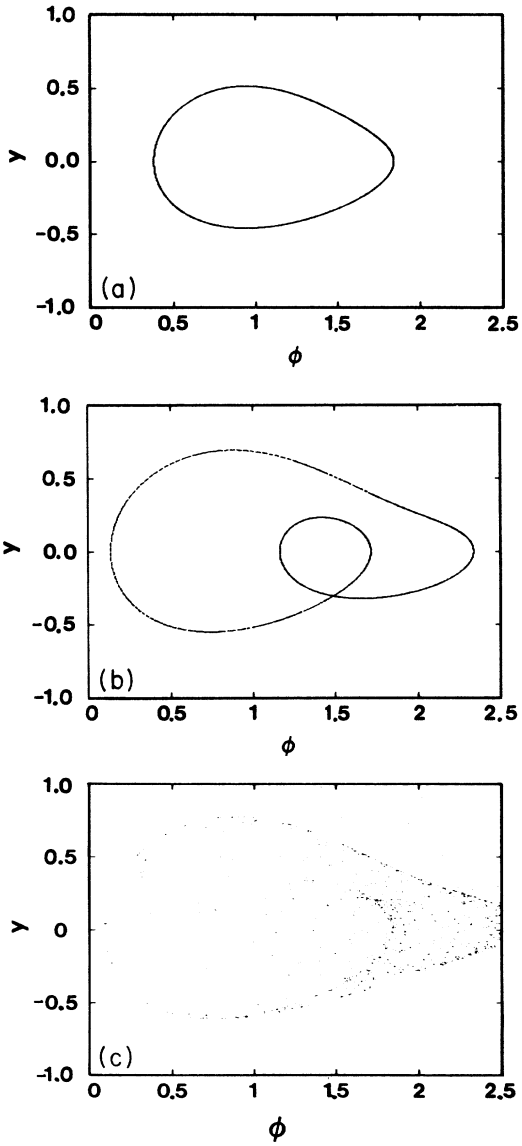

FIG. 5. Linear damping with cosϕ term: oscillational orbit for the same parameters as those in Fig. 4. (a) Period 1 orbit for $\rho_1=0.3$; (b) period 2 orbit for $\rho_1=0.4$; (c) chaotic orbit for $\rho_1=0.45$.

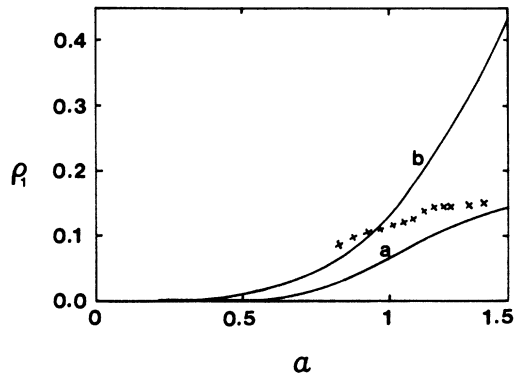

FIG. 6. Linear damping with cosϕ term: onset of chaos for $\Omega=0.4$, $\delta=-0.8$, and $\rho_0-\rho_c=0.01$. (a) The dissipative threshold; (b) the conservative threshold; crosses—onset of chaos from the numerical simulation (on rotational orbit).

In Fig. 6, a comparison of two Melnikov thresholds and the numerical result is show on the α-ρ_1 plane for $\Omega=0.4$, $\delta=-0.8$, and $\Delta\rho_0=\rho_0-\rho_c=0.01$. The numerical threshold is the lower boundary of chaos developed from the rotational orbits. It has been noticed that for $\alpha>\alpha_2=0.9$, the conservative threshold deviates quickly from the numerical result with α so that it can no longer give a good prediction for the onset of chaos. Meanwhile, the dissipative threshold is getting closer to the numerical threshold and almost coincides with it as α is increased a little further. Therefore Eq. (40) gives a better prediction on chaos for $\alpha>\alpha_2$. However, for $0.4<\alpha<0.9$, the conservative threshold is better than the dissipative threshold since the latter seems too low. For $\alpha<\alpha_1=0.4$, the two lines join together so that there is almost no difference between them. In our calculation,

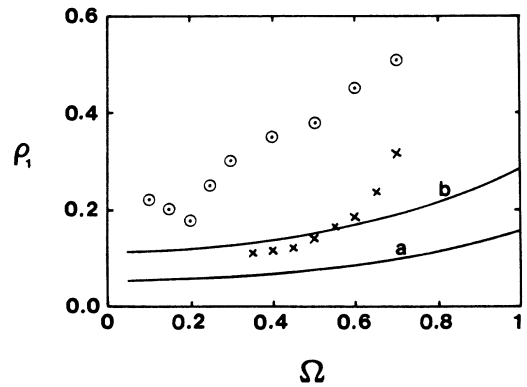

FIG. 7. Linear damping with cosϕ term: onset of chaos for $\alpha=1.004$, $\delta=-0.8$, and $\rho_0=0.8237$. The notation is the same as that in Fig. 6. ⊙—onset of chaos from the numerical simulation (on oscillational orbit).

we have also found that ρ_c is approximately the lower limit of the dc bias below which the phase-locked rotational solution cannot exist. A similar phenomenon has been discussed for the Josephson junction with only linear damping.[10]

In Fig. 7 the chaos thresholds are shown on the Ω-ρ_1 plane for $\alpha=1.004$, $\delta=-0.8$, and $\Delta\rho_0=0.01$. As we have already pointed out in Fig. 4 the system is in a periodic state with the frequency $\Omega_0=0.6873$ if the rf bias is zero. It turns out in Fig. 7 that there is no chaos at all above this frequency. When Ω approaches Ω_0 from below, the numerical threshold goes to infinite. Thus, none of these two Melnikov predictions could tell the happening of the chaos since they are finite. For $\Omega<0.55$, even though there is a noticeable discrepancy between the dissipative and the numerical thresholds, the former is still a big improvement over the conservative threshold because the Melnikov threshold has been expected to give the lower boundary of chaos for rf bias. By the way, the onset of chaos on the oscillational orbit has also been calculated numerically and shown in Fig. 7 as $\odot$. Generally, it is much higher than that on the rotational orbit and cannot be predicted by the Melnikov method.

IV. CONCLUSION AND DISCUSSION

The lack of an analytical method to predict the chaos threshold in a Josephson junction has been changed since the introduction of the Melnikov method. In general, the conservative system defined by Eq. (2) is adopted as the unperturbed system on which the Melnikov threshold is calculated. However, as Kautz and Macfarlane pointed out, the validity of the Melnikov method has been limited to the parameter region of small damping and dc bias. This situation could be greatly improved if the damping term and the dc bias are included into the unperturbed dissipative system. One such system is represented by Eq. (7) which is known to be the only one having an analytic solution. Using this solution, the following problems are studied in this paper: first, the utility of the Melnikov method has been extended to the parameter region of intermediate damping and large dc bias for the Josephson junction with quadratic damping term. It has been shown that for small damping and weak dc bias, there is no significant difference between Melnikov thresholds based on the conservative and dissipative unperturbed systems, respectively, but these two thresholds diverge from each other with the damping constant γ. For $\gamma>\gamma_1$, the latter comes close to the numerical threshold so that it yields a very good prediction of chaos, while the former seems completely useless since it is too high. This result is not difficult to understand if we recall that the Melnikov method is a perturbation method. The smaller the perturbation, the more precise the result. It is obvious that the perturbation in the dissipative case is much smaller because the main part of the damping and dc bias has been included into the unperturbed equation.

Second, we have also used the dissipative system given by Eq. (7) as the unperturbed system for the Josephson junction with linear damping and the $\cos\phi$ term because of the lack of an analytical solution of Eq. (6). The Melnikov thresholds calculated on this system and on the conservative system [Eq. (2)] are compared with the numerical simulation in several different parameter regions. We have found that for small damping these two Melnikov thresholds are almost the same. They start to bifurcate at α_1 with increasing α. For $\alpha_1<\alpha<\alpha_2$, the Melnikov threshold based on the conservative system can give a better prediction than that based on the dissipative system. Above α_2, the latter approaches the numerical threshold curve and finally coincides with it as α is increased further, while the former is becoming too high to be used. The comparison also indicated that the agreement between the Melnikov thresholds and the numerical result depends on the frequency of the rf bias Ω. When Ω approaches the plasma frequency Ω_0 from below, both Melnikov thresholds seem too low to predict the onset of the chaos. For $\Omega>\Omega_0$ no chaos has been observed in our calculations.

Finally, a less strict validity condition [Eq. (18) or (32)] for the Melnikov prediction has been proposed. Our result has verified that the satisfaction of this condition may generate better agreement between the Melnikov threshold and the numerical simulation.

ACKNOWLEDGMENTS

We are very grateful to J. Shi for many helpful discussions. This work was supported by the Texas Center for Superconductivity at the University of Houston under the prime Grant No. MDA 972-8-G-0002 to the University of Houston from DARPA and the State of Texas and a grant from the Robert A. Welch Foundation.

*Permanent address: Department of Physics, Nanjing University, Nanjing, People's Republic of China.

[1]R. L. Kautz and J. C. Macfarlane, Phys. Rev. A **33**, 498 (1986).
[2]Z. D. Genchev, Z. G. Ivanov, and B. N. Todorov, IEEE Trans. Circuits Syst. **30**, 633 (1983).
[3]V. N. Gubankov, S. L. Ziglin, K. I. Konstantinyan, V. P. Koshelets, and G. A. Ovsyannikov, Zh. Eksp. Teor. Fiz. **86**, 343 (1987) [Sov. Phys.—JETP **59**, 198 (1984)].
[4]Qian Min, Pan Tao, and Liu Zheng-Rong, Acta Phys. Sin. **36**, 149 (1989).
[5]G. Cicogna, Phys. Lett. A **121**, 403 (1987).
[6]N. F. Pedersen and K. Saermark, Physica **69**, 572 (1973).
[7]M. Bartucceli, P. L. Christiansen, N. F. Pedersen, and M. P. Soerensen, Phys. Rev. B **33**, 4686 (1986).
[8]A. J. Lichtenberg and M. A. Lieberman, *Regular and Stochastic Motion* (Springer-Verlag, New York, 1983).
[9]N. F. Pedersen, T. F. Finnegan, and D.N. Langenberg, Phys. Rev. B **6**, 4151 (1972).
[10]R. L. Kautz and R. Monaco, J. Appl. Phys. **57**(3), 875 (1985).